GPS-RO at ECMWF

Carla Cardinali and Sean Healy

ECMWF, Reading, UK
carla.cardinali@ecmwf.int

Summary

In this paper, a comprehensive assessment of the impact of radio occultation observations in the operational ECMWF assimilation and forecast system is presented using advanced diagnostic tools. In particular, the observation influence in the assimilation process and the related contribution on the short-range forecast error of radio occultation observations is evaluated with recently developed diagnostic tools based on the adjoint version of the assimilation and forecast model. The sensitivity with respect to observation error variances is also evaluated for the assimilated observations. The results indicate that a deflation of the error variances for all observation types but radiosonde and polar atmospheric motion vectors, would reduce the short range forecast error. In particular, a sensitivity analysis experiment with reduced error variance for radio occultation observations shows on average, a better fit with respect to aircraft and radiosonde measurements.

KEYWORDS: Radio occultation observations, observation error variance, adjoint diagnostic tools

1. Introduction

The ECMWF four-dimensional variational system (4D-Var, Rabier *et al.* 2000) handles a large variety of both space and surface-based meteorological observations (more than 30 million a day) and combines the observations with the prior (or background) information on the atmospheric state. A comprehensive linearized and non-linear forecast model is used, counting 10^8 the order of degrees of freedom.

The assessment of the contribution of each observation to the analysis is among one of the most challenging diagnostics in data assimilation and numerical weather prediction. Methods have been derived to measure the observational influence in data assimilation schemes (Purser and Huang 1993, Cardinali *et al*. 2004, Chapnick *et al*. 2004, Lupu *et al*. 2011). These techniques show how the influence is assigned during the assimilation procedure, which partition is given to the observation and which is given to the background or pseudo-observation. They therefore provide an indication of the robustness of the fit between model and observations and allow some tuning of the weights assigned in the assimilation system. Measures of the observational influence are useful for understanding the Data Assimilation (DA) scheme itself: the influence of e.g. the latest data on the analysis, the influence of the background, the analysis change if one single influential observation is removed or the total amount of information extracted from the available data.

It is therefore necessary to consider the diagnostic methods that have been developed for monitoring statistical multiple regression analyses; 4D-Var is, in fact, a special case of the Generalized Least Square (GLS) problem (Talagrand*,* 1997) for weighted regression thoroughly investigated in the statistical literature.

For the forecast, the assessment of the forecast performance can be achieved by adjoint-based observation sensitivity techniques that characterize the forecast impact of every measurement (Baker and Daley 2000, Langland and Baker 2004, Cardinali and Buizza, 2004, Morneau *et al*., 2006, Xu and Langlang, 2006, Cardinali 2009, Zhu and Gelaro 2009). The technique computes the variation in the forecast error due to the assimilated data. In particular, the forecast error is measured by a scalar function of the model parameters, namely wind, temperature, humidity and surface pressure that are more or less directly related to the observable quantities.

In general, the adjoint methodology can be used to estimate the sensitivity measure with respect to any assimilation system parameter of importance. For example, Daescu (2008) derived a sensitivity equation of an unconstrained variational data assimilation system from the first-order necessary condition with respect to the main input parameters: observation, background, observation and background error covariance matrices. In particular, the sensitivity with respect the observation error variance offers guidance to variances tuning beneficial to short range forecast.

A general description of the tools used is given in Section 2 on the observation influence, Section 3 on the observation impact in the forecast error and Section 4 on the sensitivity of the forecast error to the data error variance. Section 5 shows the observations performance on the ECMWF assimilation and forecast system and an assessment of the impact of GPS-RO (radio occultation) data is presented.

2. Observational influence for DA scheme

DA systems for NWP provide estimates of the atmospheric state $\mathbf{x}$ by combining meteorological observations $\mathbf{y}$ with prior (or background) information $\mathbf{x}_b$. A simple Bayesian Normal model provides the solution as the posterior expectation for $\mathbf{x}$, given $\mathbf{y}$ and $\mathbf{x}_b$. The same solution can be achieved from a classical *frequentist* approach, based on a statistical linear analysis scheme providing the Best Linear Unbiased Estimate (Talagrand, 1997) of $\mathbf{x}$, given $\mathbf{y}$ and $\mathbf{x}_b$. The optimal GLS solution to the analysis problem (see Lorenc, 1986) can be written

$$\mathbf{x}_a = \mathbf{K}\mathbf{y} + (\mathbf{I}_n - \mathbf{K}\mathbf{H})\mathbf{x}_b \tag{2.1}$$

The vector $\mathbf{x}_a$ is the 'analysis'. The gain matrix $\mathbf{K}$ ($n \times p$) takes into account the respective accuracies of the background vector $\mathbf{x}_b$ and the observation vector $\mathbf{y}$ as defined by the $n \times n$ covariance matrix $\mathbf{B}$ and the $p \times p$ covariance matrix $\mathbf{R}$, with

$$\mathbf{K} = (\mathbf{B}^{-1} + \mathbf{H}^T\mathbf{R}^{-1}\mathbf{H})^{-1}\mathbf{H}^T\mathbf{R}^{-1} \tag{2.2}$$

Here, $\mathbf{H}$ is a $p \times n$ matrix interpolating the background fields to the observation locations, and transforming the model variables to observed quantities (e.g. radiative transfer calculations transforming the models temperature, humidity and ozone into brightness temperatures as observed by several satellite instruments). In the 4D-Var context introduced below, $\mathbf{H}$ is defined to include also the propagation in time of the atmospheric state vector to the observation times using a forecast model.

Substituting (2.2) into (2.1) and projecting the analysis estimate onto the observation space, the estimate becomes

$$\hat{\mathbf{y}} = \mathbf{H}\mathbf{x}_a = \mathbf{HKy} + (\mathbf{I}_p - \mathbf{HK})\mathbf{H}\mathbf{x}_b \qquad 2.3$$

It can be seen that the analysis state in observation space ($\mathbf{Hx_a}$) is defined as a sum of the background (in observation space, $\mathbf{Hx_b}$) and the observations **y**, weighted by the $p \times p$ square matrices $\mathbf{I} - \mathbf{HK}$ and $\mathbf{HK}$, respectively.

In this case, for each unknown component of $\mathbf{H}x$, there are two data values: a real and a 'pseudo' observation. The additional term in (2.3) includes these pseudo-observations, representing prior knowledge provided by the observation-space background $\mathbf{Hx_b}$. The analysis sensitivity with respect to the observations is obtained (Cardinali et al 2004):

$$\mathbf{S} = \frac{\partial \hat{\mathbf{y}}}{\partial \mathbf{y}} = \mathbf{K}^T \mathbf{H}^T \qquad 2.4$$

The (projected) background influence is complementary to the observation influence. For example, if the self-sensitivity with respect to the *i*th observation is S_{ii}, the sensitivity with respect the background projected onto the same variable, location and time will be simply $1\text{-}S_{ii}$.

In particular, the observation influence S_{ii}=[0,1] where S_{ii}=0 means that the *i*th observation has had no influence at all in the analysis (only the background counted) and S_{ii}=1 indicates that an entire degree of freedom has been devoted to fit that data point (the background has had no influence). The tr(**S**) can be interpreted as a measure of the amount of information extracted from the observation or 'degree of freedom for signal' (DFS) whilst it follows that the complementary trace, tr(**I**–**S**)=p–tr(**S**), is the *DF* for background. That is the weight given to prior information, to be compared to the observational weight tr(**S**). Hereafter, the observation influence S_{ii} is denoted as OI. In conclusion, the DFS is a function of the observation and the background covariance matrices and the model itself as a time-spatial propagator and the observations number.

3. Forecast sensitivity to the observations

Baker and Daley (2000) derived the forecast sensitivity equation with respect to the observations in the context of variational DA. Let us consider a scalar J-function of the forecast error. Then, the sensitivity of J with respect to the observations can be written using a simple derivative chain as:

$$\frac{\partial J}{\partial \mathbf{y}} = \frac{\partial J}{\partial \mathbf{x}_a}\frac{\partial \mathbf{x}_a}{\partial \mathbf{y}} \qquad 3.1$$

$\partial J / \partial \mathbf{x}_a$ is the sensitivity of forecast error to initial condition $\mathbf{x}_a$ (Rabier et al. 1996, Gelaro et al., 1998) where the forecast error is expressed as dry energy norm. A few years ago, the use of moist norm instead of the dry one has been investigated (Barkmeijer *et al* 2001) and results have indicated that if a humidity term is considered in the final time norm, the largest norm contribution with respect to the initial analyzed fields was unrealistically provided by humidity rather than by vorticity, divergence or temperature fields. It was therefore necessary to apply an arbitrary tuning coefficient to diminish the effect. A full representation of the moist processes in the adjoint model is instead used that appropriately links the sensitivity of the forecast error with respect to the initial humidity with the sensitivity with respect to the other fields e.g. temperature.

From (2.1) the sensitivity of the analysis system with respect to the observations and the background can be derived from:

$$\frac{\partial \mathbf{x}_a}{\partial \mathbf{y}} = \mathbf{K}^T \qquad 3.2$$

By using (3.2) and (2.2) the forecast sensitivity to the observations becomes:

$$\frac{\partial J}{\partial \mathbf{y}} = \mathbf{K}^T \frac{\partial J}{\partial \mathbf{x}_a} = \mathbf{R}^{-1}\mathbf{H}(\mathbf{B}^{-1} + \mathbf{H}^T\mathbf{R}^{-1}\mathbf{H})^{-1} \frac{\partial J}{\partial \mathbf{x}_a} \qquad 3.3$$

A second order sensitivity gradient needs to be considered in 3.3 (Langland and Baker 2004; Errico 2007) because only superior orders than first contain the information related to the forecast error. In fact, the first order one only contains information on the sub-optimality of the assimilation system (Cardinali 2009).

The variation δJ of the forecast error expressed by J can be found by rearranging (3.1) and by using the adjoint property for the linear operator:

$$\begin{aligned} \delta J &= \left\langle \frac{\partial J}{\partial \mathbf{x}_a}, \delta \mathbf{x}_a \right\rangle = \left\langle \frac{\partial J}{\partial \mathbf{x}_a}, \mathbf{K}(\mathbf{y} - \mathbf{H}\mathbf{x}_b) \right\rangle = \left\langle \mathbf{K}^T \frac{\partial J}{\partial \mathbf{x}_a}, \mathbf{y} - \mathbf{H}\mathbf{x}_b \right\rangle \\ &= \left\langle \mathbf{K}^T \frac{\partial J}{\partial \mathbf{x}_a}, \delta \mathbf{y} \right\rangle = \left\langle \frac{\partial J}{\partial \mathbf{y}}, \delta \mathbf{y} \right\rangle \end{aligned} \qquad 3.5$$

where $\delta \mathbf{x}_a = \mathbf{x}_a - \mathbf{x}_b$ are the analysis increments and $\delta \mathbf{y} = \mathbf{y} - \mathbf{H}\mathbf{x}_b$ is the innovation vector. The sensitivity gradient $\partial J / \partial \mathbf{x}_a$ is valid at the starting time of the 4D-Var window (typically 09 and 21 UTC for the 12h 4D-Var set-up used at ECMWF). As for **K**, its adjoint $\mathbf{K}^{\mathrm{T}}$ incorporates the temporal dimension, and the δ**y** innovations are distributed over the 12-hour window. The variation of the forecast error due to a specific measurement can be summed up over time and space in different subsets to compute the average contribution of different component of the observing system to the forecast error. For example, the contribution of all AMSU-A satellite instruments, *s*, and channels, *i*, over time *t* will be:

$$\delta J_{AMSU-A} = \sum_{s \in S} \sum_{\substack{i \in channel \\ t \in T}} \delta J^s{}_{it} \qquad 3.6$$

The forecast error contribution can be gathered over different subsets that can represent a specific observation type, a specific vertical or horizontal domain, or a particular meteorological variable. In summary, the forecast error contribution to each measurement assimilated depends on the sensitivity to the forecast error with respect to the measurement (large absolute forecast error determines large absolute sensitivity); the adjoint of the assimilation system (which is affected by the background and the observations statistics as the model itself) and the innovation vector. When the measurements are gathered together, e.g. by instrument type, also the number will affect the observation impact.

In practice, the forecast error is computed as the difference between the 24-hour forecast and the analysis valid at the same time. This implies that the verifying analysis is considered to be the *truth*. The following aspects should be kept in mind:

- The verifying analysis is only a proxy of the truth and thus errors in the analysis can obscure problems in the short-range forecast.
- Energy norm is a suitable choice because it directly depends on the most relevant model parameters, also contained in the control vector **x**. Nevertheless, alternative functions of model parameters can be used.

4. Forecast sensitivity to the observation error variances

Daescu (2008), Daescu and Todling (2010) and Daescu and Langland (2012) have shown how the forecast sensitivity to the observation error variance can be computed. In particular, the covariance matrices can be expressed by the parametric expression

$$\mathbf{B}(s^b) = \mathbf{B}, \quad \mathbf{R}_i(s_i^{\,o}) = s_i^{\,o}\mathbf{R}_i \qquad i \in I \tag{4.1}$$

where **s** denote the (I+1)-dimensional parameter vector of error covariance weights. The vector denoted **s**=1 is obtained by setting all parameter values to 1 and corresponds to the error covariance specification **B** and **R.** The forecast sensitivity to the observation weights at **s**=1 is then expressed as

$$\frac{\partial J}{\partial s_i^{\,o}} = \frac{\partial J}{\partial \mathbf{y}_i}(\mathbf{H}_i\mathbf{x}_a - \mathbf{y}_i)^T \tag{4.2}$$

That is equivalent to

$$\frac{\partial J}{\partial \mathbf{R}} = \frac{\partial J}{\partial \mathbf{y}}(\mathbf{H}\mathbf{x}_a - \mathbf{y})^T\,\mathbf{R}^{-1} \tag{4.3}$$

The formula above has been used to compute the ECMWF forecast sensitivity to the observation weights.

5. Results

Analysis and forecast experiments using the ECMWF 4D-Var system (Rabier *et al* 2000; Janiskova *et al*. 2002; Lopez and Moreau, 2005) have been performed for June 2011 to assess the observations impact on the analysis and the forecast. Figure 1a shows the DFS of all the observations assimilated. It can be seen that AMSU-A together with AIRS radiances are the most informative data type, providing 21% of the total observational information; AIRS follows with 16%. The information content of Aircraft (9%) is the largest among conventional observations, followed by TEMP (radiosonde) and the in situ surface pressure SYNOP observations (~4%). Noticeable is the 7% of

GPS-RO (4th in the satellite *DFS* ranking). In general, the importance of the observations as defined by the *DFS* well agrees with the recent data impact studies by Radnoti *et al*, (2010).

The 24-hour forecast error contribution (FEC) of all the observing system components is shown in Fig. 1b. The largest contribution in decreasing the forecast error is provided by AMSU-A (~21%); IASI, AIRS, GPS-RO and AIREP provide 10% of the forecast error reduction followed by TEMP and SYNOP data (5%). All the other observations contribute up to 3%. AMV observations from all the different platforms (MODIS, Meteosat and GOES) also well contribute to the 24 hour error reduction (6%).

Comparing Fig. 1a with Fig. 1b is clear that the impact of the observations (by observation type) on the analysis (DFS) is quite similar to their impact on the forecast as measured by the forecast error (FEC) reduction. Both measures depend on the transpose Kalman gain matrix $\mathbf{K}^T$, FEC also depends on the forecast error and on the innovation vector. The amount of error reduction is modulated by the percentage of forecast error that projects on $\mathbf{K}^T$. For some observation types the DFS is larger than the reduction of the forecast error. The impact loss, noticed for some observation type e.g. IASI and AIRS, can depend on the observation quality or can be due to biases in the model that will prevent the analysis changes to affect the short-range forecast which will reflect on the 24 hour forecast error increase.

In Figure 1c, the sensitivity with respect to the observations error variance is shown for the same observation types. The positive sensitivities indicate that error variance deflation should be beneficial to reduce the 24 hour forecast error whilst inflation should be applied on observation error variance with negative sensitivity. According to Fig. 1c all the variances should be deflated a part for TEMP and AMV from MODIS and Meteosat. The complementary information from Fig. 1c is that the model error variances are in general too small and their inflation should be beneficial to the short range forecast.

In the ECMWF system, GPS-RO provides the 7% of DFS (Fig1a) and 10% of forecast reduction (Fig 1b). The GPS-RO measurements mainly provide temperature information in the upper-troposphere and lower/middle stratosphere. They are assimilated as bending angles, α, as a function impact parameter, a, which is a height co-ordinate, using the one dimensional observation operator described by Healy and Thépaut (2006). The GPS-RO measurements complement the information provided by satellite radiances because they have superior vertical resolution, and they can be assimilated without bias correction to the NWP model. The assumed GPS-RO observation errors used in the assimilation of the data at ECMWF vary as a function of impact height, z, which is defined as (impact parameter minus the "radius of curvature"), where the radius of curvature is radius of the best spherical fit to the earth at the location of the observation. The assumed standard deviation of the bending angle errors, $\sigma_\alpha(z)$, is 20 % of the observed value at $z = 0$ km impact height, falling linearly with impact height to 1 % at 10 km. Above 10 km, the errors are assumed to be 1 % of the observed value, until this reaches a lower limit of 3 microradians. Given the high observation accuracy, the mean GPS-RO observation influence in the analysis is also high, contributing for half to the DFS, the other half contribution comes from the relatively high number assimilated.

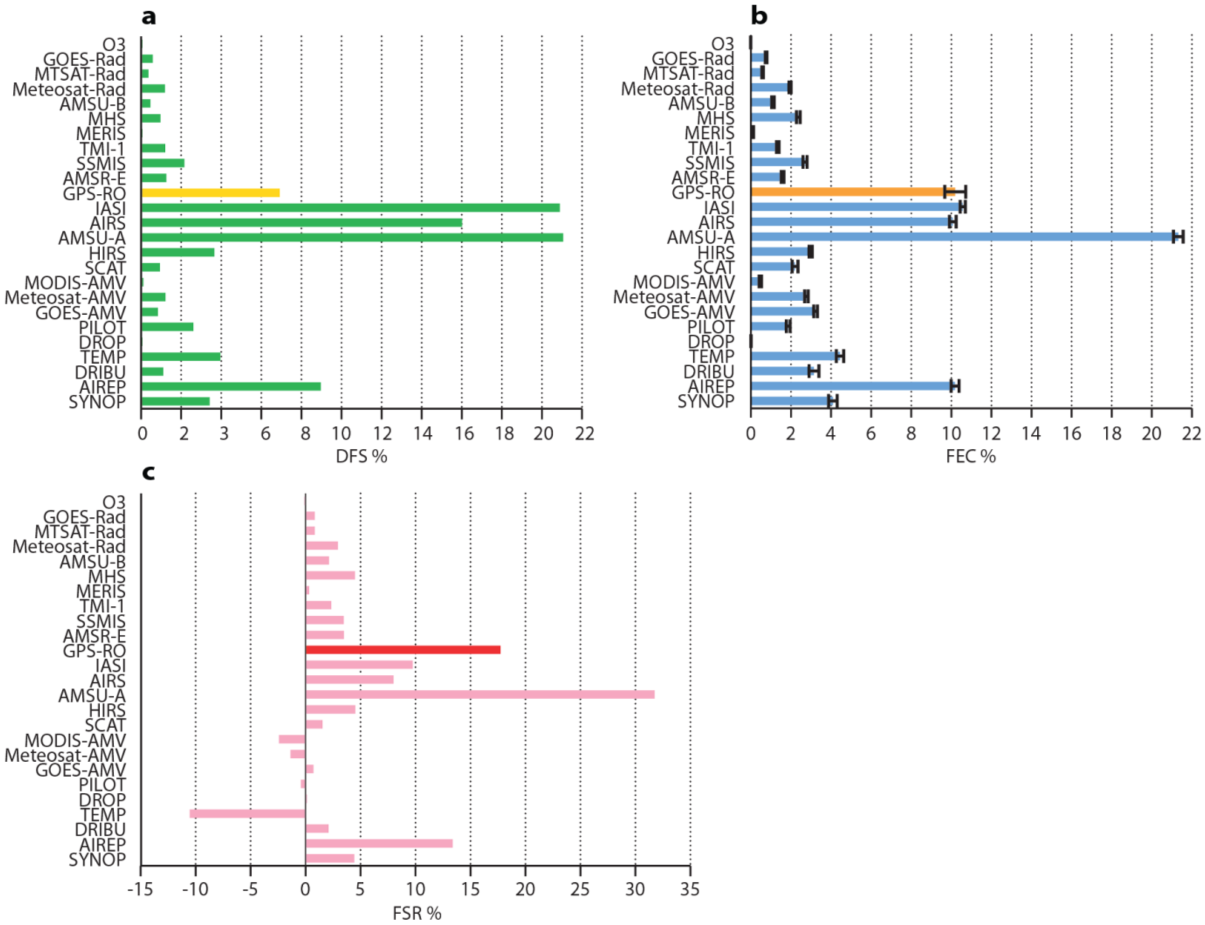

Figure 1: Total amount of a) DFS, b)FEC and c) FSR for the June 2011 and for all observation types assimilated

Figure 2 shows the mean Observation Influence (OI) (Fig. 2a) of GPS-RO data with respect to the vertical level measured in kilometres (2-50 km). The largest OI is over the troposphere and the low stratosphere where is also observed the largest forecast error reduction. The number of measurement per level is the same.

The GPS-RO OI (Fig. 2a) profiles are consistent with the earlier 1D-Var information content studies (e.g., Healy and Eyre, 2000), and reflect the large weight given to the observations between ~ 10 – 30 km. The largest forecast error reduction is also observed between 10 and 30 km (Fig. 2b). Figure 2c shows GPS-RO observations sensitivity to the observation error variance. Generally, a deflation of the variances is suggested for all vertical levels and in particular between 10 and 30 km. It is interesting to note that the FSR computation suggests reducing the assumed errors mostly in the layer where the weight given to the GPS-RO is already very large.

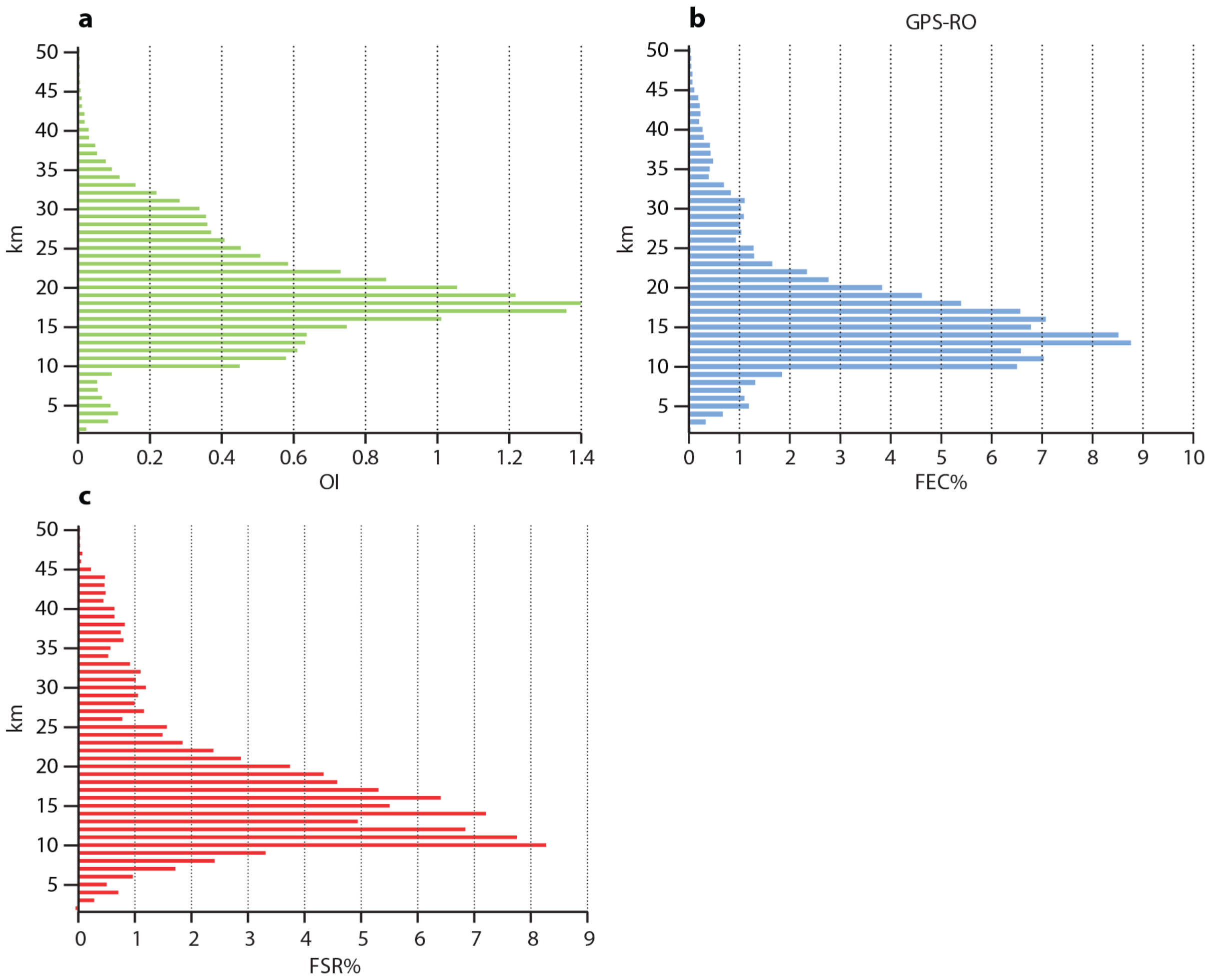

Figure 2: a) mean observation influence (OI), b) total FEC and c) FSR for June 2011 and for GPS-RO observations as a function of vertical levels

Figure 3 shows the geographical distribution of the forecast error reduction due to GPS-RO data (Fig.3a) and the forecast sensitivity to the GPS-RO observation error variance (Fig. 3b) averaged between 12 and 20 km and for June 2011.

The average mean forecast impact of GPS-RO is larger over the Tropics area than in the extra-tropic (Fig 3a blue contour) but in general, a part few areas of degradation close to the poles, the GPS-RO observations decrease the 24 hour forecast error everywhere. As can be seen from Fig.3b, the largest signal for observation error variance reduction is also in the tropical area (yellow-red contours).

An analysis sensitivity experiment *Half_Sigma* has been performed by reducing the GPS-RO error variance. In particular, the GPS-RO error variance deflation profile suggested by the FSR computation was approximated with the analytical expression

$$\sigma^*_\alpha(z) = \sigma_\alpha(z) \times (1 - \gamma\, \mathbf{exp}(1 - (z - z_m)/H - \mathbf{exp}(-(z - z_m)/H)),$$

where $z_m = 15\text{km}$ and $H = 2.5\,\text{km}$. The parameter γ was set to 0.5 for the 50 % reduction in the errors.

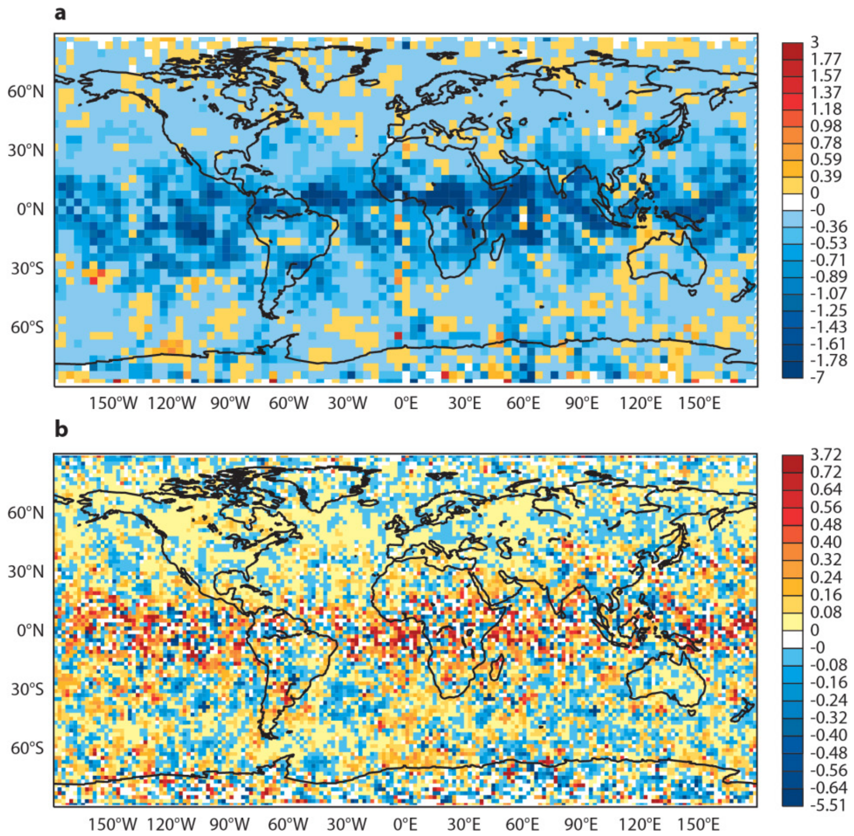

Figure 3: GPS-RO a) mean FEC and b) mean FSR for June 2011 from 12 to 30 km. (a) Positive (negative) values mean increase (decrease) of forecast error. (b) Positive (negative) values mean that deflation (inflation) of the observation error variances would decrease the 24 hour forecast error.

The performance of *Half_Sigma* has been compared with the performance of the control (CNTR) experiment which contains the operational assigned variances $\sigma_a(z)$. The performance has been measured in term of observation fit. Figure 4 shows the mean forecast differences with respect to radiosonde observations of 24 (solid line) and 48 (dot line) hour forecast range for CNTR (black) and *Half_Sigma* (red) for June 2011 and for the u-component (left panel), v-component (middle panel) and t (right panel)

Half_Sigma indicates a mean improvement with respect to the radiosonde fit especially for the 48 hour forecast range at every level. The best improvement is noticed in the high troposphere and lower stratosphere and for the u and v component. When the experiments are compared with the aircraft observations a larger fit reduction is noticed in *Half_Sigma* than in CNTR for the 48 hour range forecast in the troposphere for the u component of the wind in the Tropics (Fig 5a) and the Southern Hemisphere (Fig 5b).

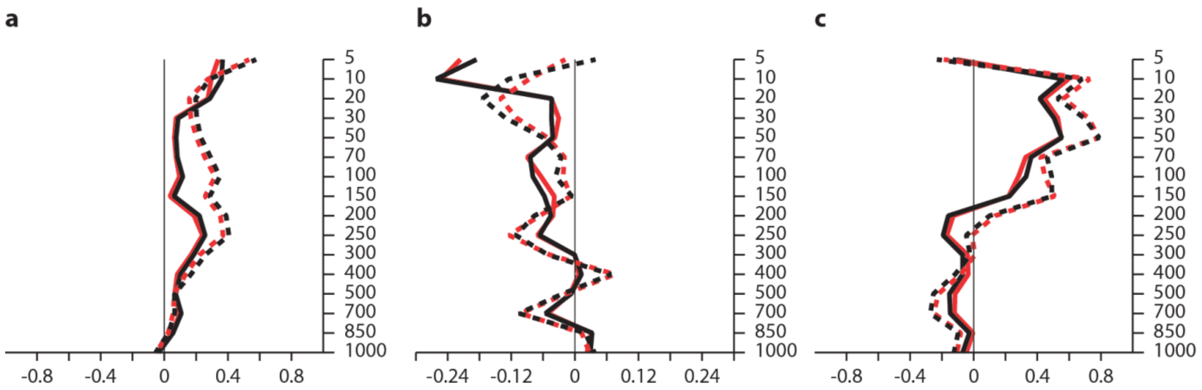

Figure 4: Mean forecast differences with respect to radiosonde observations of 24 (solid line) and 48 (dot line) hour forecast range for CNTR (black) and Half_Sigma (red) for June 2011 and for the u-component ((a left panel), v-component ((b) middle panel) and t ((c) right panel) in the Northern Hemisphere.

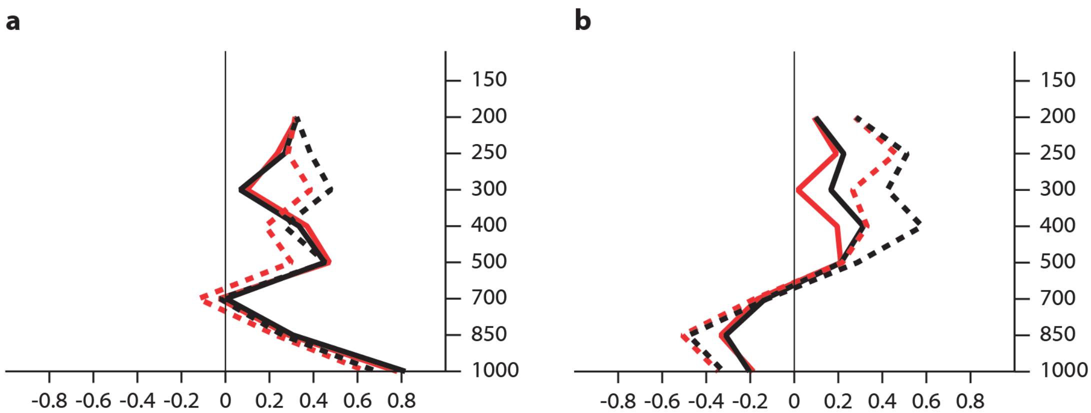

Figure 5: Mean forecast differences with respect to radiosonde observations of 24 (solid line) and 48 (dot line) hour forecast range for CNTR (black) and Half_Sigma (red) for June 2011 and for the u-component in the Tropics (top panel) and Southern Hemisphere (right panel)

6. Conclusions

Over the last few years, the potential of using derived adjoint-based diagnostic tools has been increasingly exploited.

The influence matrix is a well-known concept in multi-variate linear regression, where it is used to identify influential data and to predict the impact on the initial condition estimates of removing individual data from the regression. The self-sensitivity provides a quantitative measure of the observation influence in the analysis. In the context of 4D-Var there are many components that together determine the influence given to any one particular observation. First there is the specified observation error covariance **R**, which is obtained simply from tabulated values. Second, there is the background error covariance **B**, and third, the dynamics and the physics of the forecast model which propagate the covariance in time, and modify it according to local error growth in the prediction. The total influence is further modulated by data density.

Forecast sensitivity to observations can be used to diagnose the impact on the short-range forecast, namely 24 to 48 hours, given the use of a simplified adjoint of the data assimilation (DA) system and the implied linearity assumption. Forecast error contribution maps allow the geographical identification of beneficial or detrimental observation impact and a clear understanding of the causes can be drawn by the help of observing system experiment (OSE) in which the data of interest are denied. In general, OSEs are also used to investigate forecast data impact on a longer range forecast, typically 5 days.

The global impact of observations is found to be positive and the forecast errors decrease for all data types. The largest contribution in the analysis as measured by the DFS and in the forecast as measured by FEC is provided by microwave sounder radiances (AMSU-A) followed by the infrared sounder radiances (IASI and AIRS) from the instruments that mainly provide information on temperature and humidity. For microwave satellite humidity information, SSMIS (microwave imager), MHS (microwave sounder) and AMSR-E (microwave imager) instruments are in this order contributing to forecast error decrease. For conventional observations Aircraft and Temp provide the largest contribution. The forecast sensitivity to the observation variance suggests that if the observation error variances for all observation type, but Temp and AMV, are deflated, the 24 hour forecast error will reduce.

The 5th largest impact either in the analysis or in the forecast is provided by GPS-RO data. The largest contribution comes from the vertical levels between 12 and 20 km. The forecast sensitivity to the observation error variances also suggests that the GPS-RO weights should be deflated to reduce the forecast error. Interestingly, the suggested reduced variances are mostly in the layer where the weight given to the GPS-RO is already quite large. A first attempt to decrease the GPS-RO observation error variances has been made and some improvement in terms of observation fit has been noticed. Anyhow, more work is envisaged to properly tune the variances for GPS-RO and in general for all the other observation types.

Acknowledgements

The authors thanks Els Kooij-Connally who very patiently waited for the manuscript to be delivered

References

Baker N.L. and R. Daley, 2000: Observation and background adjoint sensitivity in the adaptive observation targeting problem. *Q. J. R. Meteorol. Soc*, **126**,1431—1454

Barkmeijer J., R. Buizza, T. N. Palmer, K. Puri and J.-F. Mahfouf, 2001: Tropical singular vectors computed with linearized diabatic physics. *Q. J. R. Meteorol. Soc.*, **127**, 685—708

Bauer, P., A. J. Geer, P. Lopez, and D. Salmond, 2010: Direct 4D-Var assimilation of all-sky radiances: Part I. implementation. *Q. J. R. Meteorol. Soc*., **136**, 1868—1885

Cardinali, C., and R. Buizza: 2004. Observation sensitivity to the analysis and the forecast: a case study during ATreC targeting campaign. Proceedings of the First THORPEX International Science Symposium, 6-10 December 2004, Montreal, Canada, WMO TD 1237 WWRP/THORPEX N. 6.

Cardinali, C., S. Pezzulli and E. Andersson, 2004: Influence matrix dagnostics of a data assimilation system. *Q. J. R. Meteorol. Soc.*, **130,** 2767—2786

Cardinali, C, 2009: Monitoring the forecast impact on the short-range forecast. *Q. J. R. Meteorol. Soc.*, **135,** 239—250.

Chapnik, B., G. Desrozier, F. Rabier and O. Talagrand, 2004: Property and first application of an error-statistics tuning method in variational assimilation. *Q. J. R. Meteorol. Soc.*, **130,** 2253—2275.

Chapnik, B., G. Desrozier, F. Rabier and O. Talagrand, 2006: Diagnosis and tuning of observation error in a quasi-operational data assimilation setting. *Q. J. R. Meteorol. Soc.*, **132,** 543—565.

Daescu, D.N., 2008: On the sensitivity equations of four-dimensional variational (4D-Var) data assimilation. *Mon. Wea. Rev.*, **136**, 3050-3065.

Daescu, D. N. and Langland, R. H., 2012: Error covariance sensitivity and impact estimation with adjoint 4D-Var: theoretical aspects and first applications to NAVDAS-AR. *Q.J.R. Meteorol. Soc.*. doi: 10.1002/qj.1943.

Daescu, D. N. and Todling, R., 2010: Adjoint sensitivity of the model forecast to data assimilation system error covariance parameters. *Q.J.R. Meteorol. Soc.*, **136**: 2000–2012. doi: 10.1002/qj.693

Desroziers G. and Ivanov S. 2001: Diagnisis and adapting tuning of observation error parameters in a variational assimilation. *Q. J. R. Meteorol. Soc.*, **122,** 1433—1452

Errico, R., 2007: Interpretation of an adjoint-derived observational impact measure. *Tellus*, **59A**, 273-276.

Fisher, M., 2003: Estimation of entropy reduction and degrees of freedom for signal for large variational analysis systems. *ECMWF Tech. Memo.*, **397,** pp 18.

Geer, A. J., P. Bauer, and P. Lopez, 2010: Direct 4D-Var assimilation of all-sky radiances: Part II. Assessment. Quart. J. Roy. Meteorol. Soc., **136**, 1886—1905.

Geer, A.J., and P. Bauer, 2010: Enhanced use of all-sky microwave observations sensitive to water vapour, cloud and precipitation. ECMWF Tec Memo n.620

Gelaro R, R.Buizza, T.N. Palmer and E. Klinker, 1998: Sensitivity analysis of forecast errors and the construction of optimal perturbations using singular vectors. *J. Atmos. Sci.*, **55**, 1012—1037.

Hollinger, J., J. Peirce, and G. Poe, 1990: SSM/I instrument evaluation. IEEE Trans. Geosci. Remote Sensing 28, 781–790.

Healy, S.B. and J.R. Eyre, 2000: Retrieving temperature, water vapor and surface pressure information from refractive–index profiles derived by radio occultation: A simulation study. *Q.J. R. Meteorol. Soc.*, **126,** 1661—1683.

Healy, S.B. and J.-N. Thépaut, 2006: Assimilation experiments with CHAMP GPS radio occultation measurements*. Q.J. R. Meteorol. Soc.*, **132,** 605—623.

Janiskova, M., J.-J. M. J.-F. Mahfouf, and F. Chevallier, 2002: Linearized radiation and cloud schemes in the ECMWF model: Development and evaluation, *Q. J. R. Meteorol. Soc*., **128**, 1505—1527.

Langland R. and N.L Baker., 2004: Estimation of observation impact using the NRL atmospheric variational data assimilation adjoint system. *Tellus,* **56A,** 189—201.

Kawanishi, T., T. Sezai, Y. Ito, K. Imaoka, T. Takeshima, Y. Ishido, A. Shibata, M. Miura, H. Inahata and R. Spencer (2003). The Advanced Microwave Scanning Radiometer for the Earth Observing System (AMSR-E), NASDA's contribution to the EOS for global energy and water cycle studies. IEEE Trans. Geosci. Remote Sensing **41**, 184—194.

Lorenc, A., 1986: Analysis methods for numerical weather prediction. *Q. J. R. Meteorol. Soc*., **112,** 1177—1194.

Lopez, P. and E. Moreau, 2005: A convection scheme for data assimilation: Description and initial tests. *Q.J.R.Meteorol.Soc*., **131**, 409—436

Morneau J, S. Pellerin, S. Laroche, and M. Tanguay, 2006: Estimation of the adjoint sensitivity gradient in observation space using the dual (PSAS) formulation of the Enviroment Canada operational 4DVar. Proc. Second THORPEX international science symposium, 4-8 Dec 2006, Landshut Germany. WMO TD N.1355 WWRP/THORPEX No.7

Purser, R. J. and H.-L. Huang,1993: Estimating Effective Data Density in a Satellite Retrieval or an Objective Analysis. *J. Appl. Meteorol.*, **32,** 1092—1107.

Rabier, F., E. Klinker, P. Courtier, and A. Hollingsworth, 1996: Sensitivity of forecast errors to initial condition. *Q. J. R. Meteorol. Soc*. **122**, 121—150

Rabier, F., H. Järvinen, E. Klinker, J.F. Mahfouf, and A. Simmons, 2000: The ECMWF operational implementation of four-dimensional variational assimilation. Part I: experimental results with simplified physics. *Q. J. R. Meteorol. Soc*. **126,** 1143—1170.

Rodwell, M. and T. Jung, 2008: The ECMWF 'Diagnostics Explorer': A web tool to aid forecast system assessment and development. *Ecmwf Newsletter,* No 117, 21-29.

Talagrand, O., 1997: Assimilation of observations, an Introduction. *J. Meteorol. Soc. Japan*, **Vol 75,** N.1B, 191—209.

Zhu, Y. and R. Gelaro, 2008: Observation Sensitivity Calculations Using the Adjoint of the Gridpoint Statistical Interpolation (GSI) Analysis System. *Mon. Wea. Rev.*, **136,** 335—3

Xu, L., R. Langland, N. Baker and T. Rosmond, 2006: Development of the NRL 4D-Var data assimilation adjoint system. Operational Numerical Weather Prediction and Data Assimilation, European Geosciences Union, *General Assembly 2006*, Vienna, Austria, 02 – 07 April 2006.